Pergamon

Cement and Concrete Research 30 (2000) 931–936

CEMENT AND CONCRETE RESEARCH

The influence of the superplasticizer on the hydration and freezing processes in white cement studied by ^{1}H spin-lattice relaxation time and single point imaging

J. Tritt-Goc[a,*], N. Piślewski[a], S. Kościelski[b], F. Milia[c]

[a]*Institute of Molecular Physics, Polish Academy of Sciences, Smoluchowskiego 17, 60-179 Poznań, Poland*
[b]*Faculty of Technical of Physics, Poznań University of Technology, Piotrowo 3, 60-965 Poznań, Poland*
[c]*NCSR Demokritos, Institute of Materials Sciences, 153 10 Ag. Paraskevi Attiki, Athens, Greece*

Received 10 September 1999; accepted 28 March 2000

Abstract

The influence of the superplasticizer Sikament 92 on the hydration process of white cement paste and freezing behavior of hardened white cement was investigated by ^{1}H spin-lattice relaxation and Single Point Imaging (SPI) methods. The study shows that this superplasticizer extends the workability of the cement paste by about 5 h and significantly increases the hydration rate when compared with pure sample. The pore structures in hardened cement were studied by MRI and demonstrate that Sikament 92 lowers the porosity and increases resistance to freezing.

Keywords: Hydration; Microcraking; Cement; Superplasticizer

1. Introduction

The hydration and hardening of cement paste, as well as the freeze/thaw behavior of hardened cement, has been the subject of extensive study by different techniques due to the importance of cement in construction and material engineering. Among these techniques, NMR, mostly proton spin-lattice relaxation time has proved to be a powerful tool in the study of cement systems [1–9], particularly when used in conjunction with microimaging NMR techniques (MRI) [10–14]. The relaxation time measurements give the information about the hydration rate of cement and the porous structure, which is formed during the hydration. MRI has been used as a non-invasive method to monitor water distribution during the hydration process of cement or concrete paste and the pore size distribution in the freezing experiment on hardened concrete at the micro-milimetric level [14,15]. The main goal of these studies is to characterize water dynamics in cement paste and to elucidate the mechanisms responsible for the deterioration of the cement. On the other hand, the studies also give the information of the parameters which influence the mechanical properties such as workability of the cement paste, strength, durability and resistance to freezing of the hardened cement. The mechanical properties are very important from the practical point of view and a big effort from scientists is made to improve them in order to fulfill all the demands of the customers, simply to produce better cement and concrete. One of the ways to improve the mechanical properties of the cement is to add the superplasticizer, which plays an important role in the properties of setting time and development of strength in cement and in the pore structure [16,17].

In this paper, the investigations of the effect of superplasticizer Sikament 92 on the hydration process of white cement paste and freezing behavior of hardened white cement are presented. The proton spin-lattice relaxation time measurements were performed on a Bruker SXP 4/100 at 90 MHz and two-dimensional

* Corresponding author. Tel.: +48-61-8612-426; fax: +48-61-8684-524
E-mail address: jtg@ifmpan.poznan.pl (J. Tritt-Goc).

0008-8846/00/$ – see front matter
PII: S0008-8846(00)00270-2

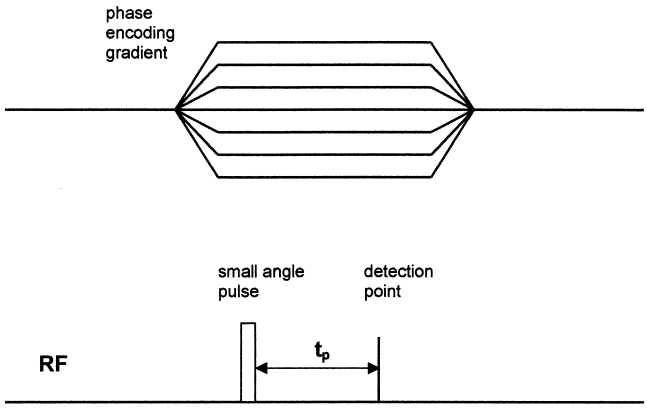

Fig. 1. A schematic description of 1D SPI sequence. A RF pulse exciting transverse magnetisation which is phase-encoding for time t_p. A single data point is sampled with quadrature at each gradient value.

(2D) MRI images were taken on a Bruker AVANCE 300 MHz.

2. Theory

The hydration process is a complex reaction of water with different component of cement [17,18]. During this reaction, the hydration products are formed which contain various forms of water such as absorbed water, pore water and bound water. They are characterized by different proton relaxation times. Thus, it is clear that the relaxation in such a complex system as cement follows the stretched exponential form:

$$M(\tau) = M_0\{1 - 2\exp[-(\tau/T_{1av})^{\alpha}]\}. \quad (1)$$

For the first time, Eq. (1) was introduced as the description of viscoelasticity and then used for a very wide range of phenomena and materials [19] among them for cement [2]. The parameter T_{1av} is the average proton spin-lattice relaxation time of protons being in different environments in cement and α is the stretched exponential parameter, which corresponds to a fractal geometry of the pore structure [5]. We used Eq. (1) in the interpretation of our experimental data. The MRI method called Constant Time Imaging (CTI) or Single Point Imaging (SPI) [20] has been proved to be the ideal method for imaging the hydration and freezing processes of cement [10–12]. A schematic description of 1D SPI method is shown in Fig. 1. In this sequence, in order to generate transverse magnetization, a short, intense and nonselective radiofrequency (RF) pulse is applied. A single data point is sampled in quadrature a fixed time t_p after the RF pulse. The spatial dimension is phase-encoded by cycling the gradient amplitude along x, y or z direction. Because there is no frequency encoding gradient, the SPI images are free from distortions due to the magnetic field inhomogenity, susceptibility variations and chemical shift. The RF pulse is applied while the phase-encoding gradient is on as is shown in Fig. 1. Thus, the duration of the pulse must be short enough to cover the range of frequency introduced by the gradient.

3. Experimental

For T_1 NMR relaxation study, two cement samples of cylindrical shape (7 mm in diameter, 10 mm in length) were prepared using white cement from Titan Cement in Greece. The first sample (W1F) contained no superplasticizer and was used as a reference sample. The second one (W1S) contained 1% of superplasticizer Sikament 92 from Switzerland, which is the aqueous solution of the sodium salt of a polycarboxylic acid-based, sulphonated vinyl co-polymer. The W1F sample was prepared by mixing distilled water with cement powder in ratio of w/c = 0.4. In the case of the second sample (W1S), the solution to cement ratio, after adding superplasticizer, was kept also at 0.4. The fresh

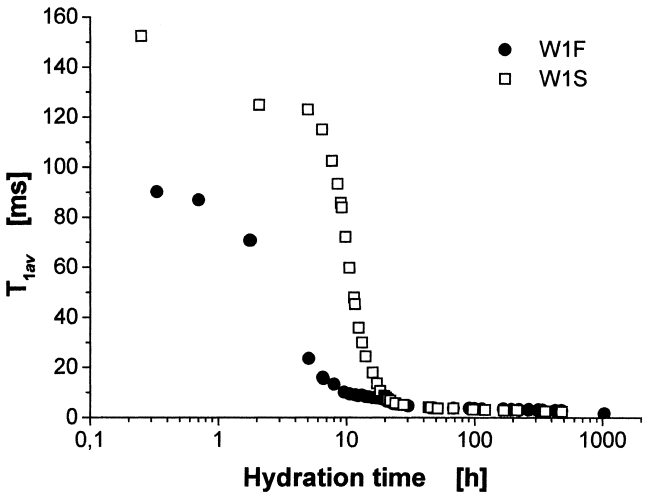

Fig. 2. Proton spin-lattice relaxation time T_{1av} as a function of the hydration time for the two samples: W1F — white cement paste, and W1S — white cement paste containing 1% of superplasticizer.

cement pastes W1F and W1S were placed in glass vials, closed with Teflon cork and parafilm so that the total water content was constant during the setting of the cement paste. T_1 measurements were performed on a Bruker SXP 4/100 spectrometer operating at a proton frequency of 90 MHz using the inversion-recovery method with short (4–8 μs) RF pulses. In the late state of the hydration process in both samples, the multiexponential relaxation behavior of the inversion curve is observed. In order to include all significant components of magnetisation recovery, every curve was measured with 70 different time increments. The measurements were done at room temperature and were performed for the time of hydration range from about 0.2 to 1000 h in time intervals from minutes to days. The freeze experiment was performed on the same samples as proton-spin-lattice relaxation time after 4 months; thus the cement paste had time to dry. After this time, the tubes with the hardened W1S and W1F samples were filled with water and small pressure was applied to assist the diffusion of the water into the cement. Therefore, the pores which normally contain air, became filled with water. The non-frozen water distribution in the samples was followed by taking images on a Bruker AVANCE 300 MHz WB spectrometer (^{1}H), equipped with a microimaging accessory, a 7-T vertical bore superconducting magnet and the temperature control unit. The images were taken as a function of temperature by lowering the temperature from 20°C to −70°C with the SPI method. A series of 2D (64 × 64) images of hardened white pure cement sample — W1F, were taken with the phase encoding time t_p equal to 85 μs, the repetition time TR of 50 ms and with a field of view (FOV) of 1.3 × 0.9 cm. These give an in-plane resolution of 203 × 140 μm. For the sample with superplasticizer — W1S, 2D (124 × 64) images were taken with the resolution of 101 × 140 μm, t_p = 118 μs, and others parameters as for the W1F sample.

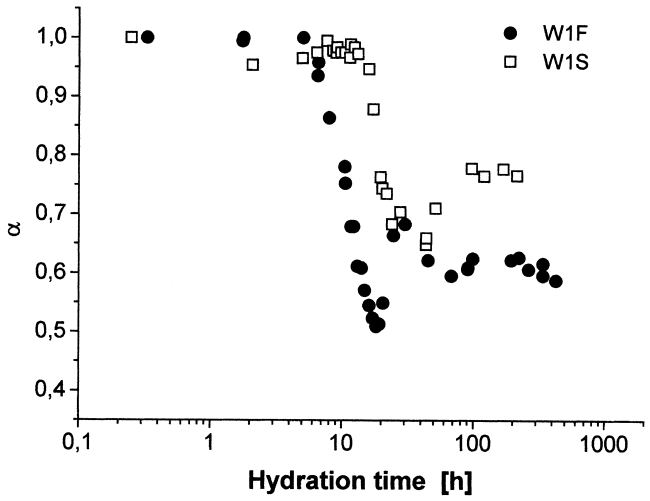

Fig. 3. Dependence of the stretched exponential exponent α on the hydration time for W1F and W1S cement paste samples.

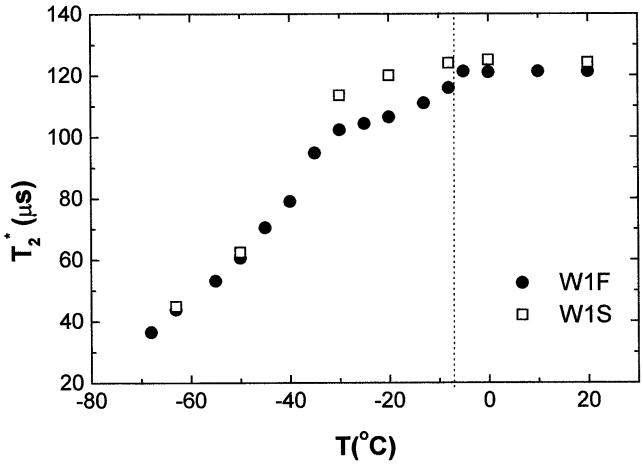

Fig. 4. Evolution of the T_2* of the pore water as a function of temperature for hardened cement samples: white cement (W1F) and white cement contained 1% of superplasticizer (W1S).

4. Results and discussion

4.1. The hydration process

The hydration of the samples was monitored by ^{1}H NMR spin-lattice relaxation time T_{1av} and the stretching parameter α by the time evolution of these parameters for pure cement sample (W1F) and the sample contained 1% of superplasticizer Sikament 92 (W1S). The results are presented in Figs. 2 and 3. In Fig. 2, the T_{1av} curves in both samples show similar behaviour: during the first stage of hydration, the "dormant period," T_{1av} is almost constant and then starts to smoothly decrease until it reaches its "final" value of about 1 ms at late stages of hydration. The shortening of T_{1av} in cement paste during thickening is attributed to the progressive increase of the solid–liquid surface. However, the addition of superplasticizer in white cement affects hydration significantly. First of all, the cement sample with superplasticizer has a longer initial T_{1av} plateau, which corresponds to a longer final setting time. For the W1S sample, the dormant period lasts about 6 h whereas for W1F, only about 0.7 h. During this time, the cement paste maintains its workability. Therefore, the lengthening of the setting time is a very important fact, which affects the demands of the customers. In addition, T_{1av} value of the dormant period in the W1S sample is higher when compared to the corresponding pure white cement sample — W1F: about 150 to 90 ms, respectively. This should be attributed to more free water in the W1S sample and prove the liquefying properties of the Sikament 92 as in others superplasticizers. The hydration rate, corresponding to the slope of the T_{1av} curves, is also affected by the superplasticizer and significantly increases when compared with the rate of the pure sample (Fig. 2).

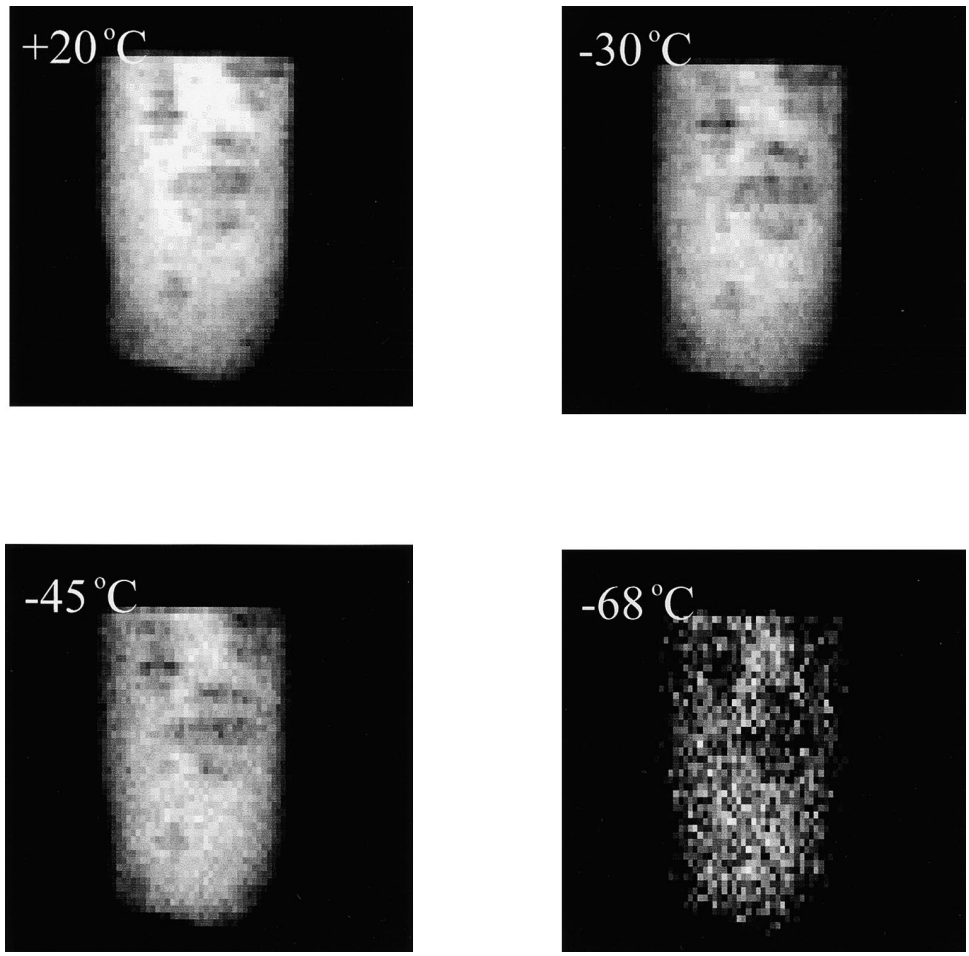

Fig. 5. A set of 2D microimages which demonstrates freezing of water occupied pores into the hardened white cement (W1F). The parameters for the images are: t_p = 85 μs, TR = 50 ms and resolution 203 × 140 $(\mu m)^2$. Greater signal intensities are represented by whiter pixels. Changes in contrast reflect the local non-frozen water content.

The evolution of the stretching parameter α as a function of hydration time for W1F and W1S samples is presented in Fig. 3. Compared to the T_{1av} results from Fig. 2, it can easily be seen that during the first hours of hydration of cement paste, the time evolution of α is analogous to T_{1av}. First, there is an almost constant value for α in the dormant period — about 1, then this parameter decreases smoothly to the value $\alpha \approx 0.5$ and 0.64 for W1F and W1S samples, respectively. Such behaviour can be explained in terms of the fractal nature of the pore size and surface-to-volume distribution in cement gel. For $\alpha = 1$, the volume fractal dimension is 3, the surface fractal dimension is 2 and the magnetisation recovery function is monoexponential. In the later stage of hydration, the gel surface becomes fractal with the fractal dimension of about 2.6 [18]. This time behaviour of the stretched exponential exponent α observed for our samples is in agreement with the results obtained also for white cement by Jarh et al. [5]. However, in contradiction to these results, in our samples at 19 and 40 h for W1F and W1S samples, respectively, we observed an increase in the value of α, than a decrease and later a renewed increase. Since the stretching parameter is an indication of the distribution of pores occupied by water, we conclude that the "unusual" behaviour observed in Fig. 3 is due to the change in structure of the hydrated cement paste matrix, most likely due to the microcracking. Such microcracking was suggested by Beyea [11]. The superplasticizer affects the creation of the pore structure in the cement. As can be seen in Fig. 3, the fractal nature of the pore size and surface-to-volume distribution in cement gel starts to develop later in the sample with superplasticizer after 18 h, whereas in the pure sample it already starts to develop after 5 h. What seems to be more important is the minimum value of α which is equal 0.5 and 0.65 for W1F and W1S, respectively. This means that Sikament 92 lowers the porosity. This is a very important property of the superplasticizer under study because the cement paste weakness is mainly associated with its porosity and in

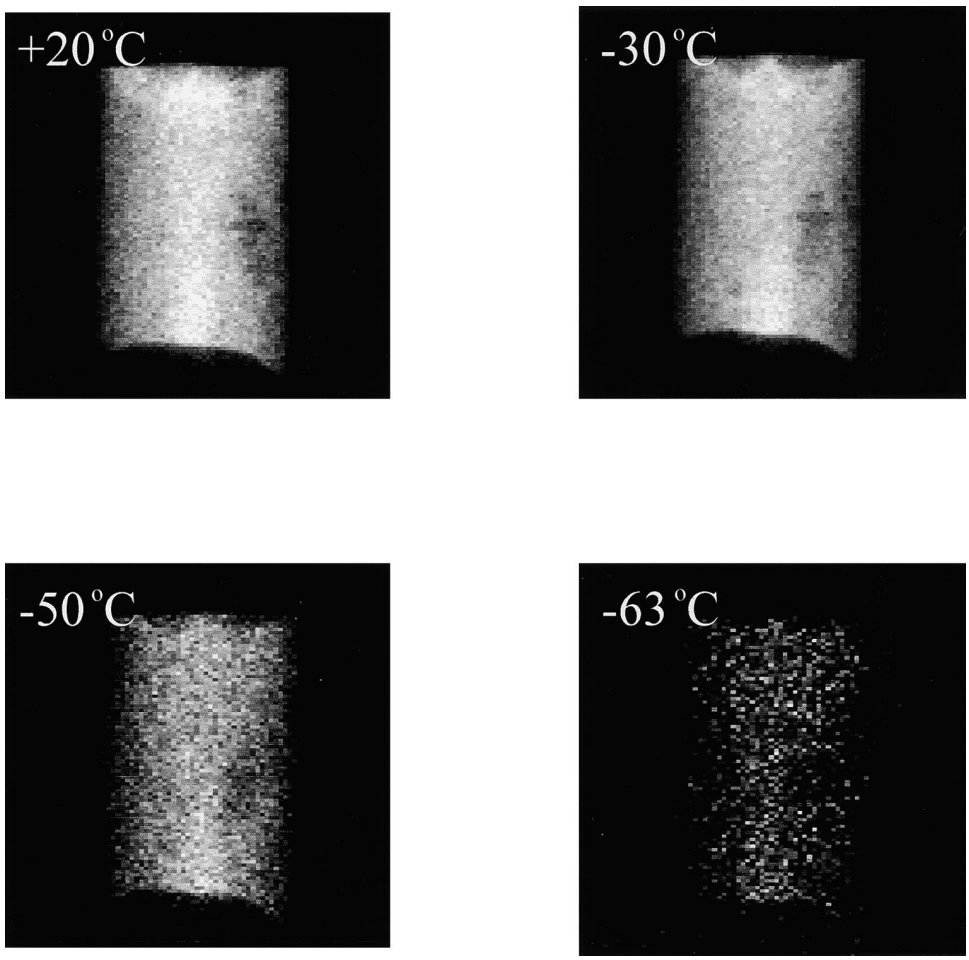

Fig. 6. A set of 2D microimages which demonstrates freezing of water occupied pores into the hardened white cement containing 1% of superplasticizer (W1S). The parameters for the images are: t_p = 118 μs, TR = 50 ms and resolution 101 × 140 (μm)^2. Greater signal intensities are represented by whiter pixels. Changes in contrast reflect the local non-frozen water content.

order to improve the mechanical properties, the porosity has to be reduced.

4.2. The white cement freeze process

The freezing behavior of the pores' water was followed by the temperature dependence of the parameter T_2* and 2D SPI images of the two hardened white cement samples W1F and W1S. A set of 16 FIDs spectra and 2D images was acquired of both samples over the temperature range from 20°C to −70°C. The samples were kept at each temperature about 20 min and then the measurements were performed. The frozen water has a short relaxation time (T_2* ≅ 10 μs) and therefore the signal of this water is invisible to the detection systems, for both the signal pulse FID (dead time of the probe longer than T_2*) and SPI sequence (t_p = 85 and 118 μs). Thus, we observed only the signal from the non-frozen water in the samples. After fitting the FID FT to Lorentzian line shapes, the parameter T_2* was calculated and the results are shown in Fig. 4. As can be seen from this figure, the water inside the pore structure of the samples remains liquid well below the normal freezing point of the ordinary bulk water [15]. Generally, the pore system in hydrated cement covers a wide range of different pore radii from macro pores through capillary to gel pores [8]. The pores' dimensions are highly influenced by the cement composition and by the hydration and drying processes. In Fig.4 for the W1F sample, we observe the first freezing point at about −8°C. At this temperature, macro water freezes. After the macro water has been frozen, the next freezing point at −30°C is related to capillary pores. Water occupying gel pores will freeze only at very low temperature, well below −100°C and we do not observe this effect. For the W1S sample, there is only one significant freezing point at −30°C, which corresponds to freezing of the capillary pores. The temperature dependence T_2* for W1S sample does not provide evidence of the freezing point related to the macro pore. Therefore, we can conclude that the pore system of cement in sample W1S was highly affected by superplasticizer Sikament 92 and that this sample is characterized by lower average dimensions of pores which gives a

higher strength and durability when compared with pure white cement sample W1F.

The SPI method is the only one which allows to follow the pore size distribution in the cement directly. The examples of a series of 2D images of hardened white pure cement sample — W1F and hardened cement samples with 1% of Sikament 92 are presented in Figs. 5 and 6, respectively. Greater signal intensities are represented by whiter pixels. Changes in contrast reflect the local non-frozen water content. We can conclude that in both samples, we observe non-homogeneous distribution of the pores water.

5. Conclusions

The time dependencies of the spin-lattice relaxation times of protons and the stretching parameter α in the function of hydration process of the white cement paste as well as the freezing experiments of the hardened white cement presented in this paper clearly show that the superplasticizer Sikament 92 can influence the quality of cement. After adding this superplasticizer, the cement paste maintains its workability for a longer time when compared with a pure sample and also the durability of the cement increases. In the hardened cement sample with Sikament 92, resistance to freezing grows. Our results proved that 2D SPI images of the hardened cement under freezing conditions can be used to study the non-frozen water distribution in the sample with very short relaxation time. Therefore, we can follow the pore structure and distribution during the freezing of cement. First, the macro pores freeze then the capillary pores. The superplasticizer influences the structure of the pores. In conclusion, our results show that the NMR relaxation combined with MRI could be considered as very powerful methods to investigate the role of superplasticizers on the hydration properties of cement paste and freezing process of hardened cement.

Acknowledgments

This work was supported by the Polish Committee for Scientific Research under project No. 2 P203B 120 14 and partially by NATO grant No. HTECH.LG 97/363.

References

[1] R. Blinc, G. Lahajnar, S. Zumer, M.M. Pintar, Nmr study of the time evolution of fractal geometry of cement gels, Phys Rev B, 38 (1988) 2873–2878.

[2] T. Kosmac, G. Lahajnar, A. Sepe, Proton nmr relaxation study of calcium aluminate hydration reactions, Cem Concr Res, 23 (1993) 1–6.

[3] R.L. Kleinberg, M.A. Horsfield, Transverse relaxation processes in porous sedimentary rock, J Magn Reson, 88 (1990) 9–19.

[4] J.J. Attard, S.J. Doran, N.J. Herrod, T.A. Carpenter, L.D. Hall, Quantitative NMR spin-lattice-relaxation imaging of brine in sandstone reservoir cores, J Magn Reson, 96 (1992) 514–525.

[5] O. Jarh, A. Sepe, G. Lahajnar, N. Koprivec, R. Blinc, M.M. Pintar, F. Milia, Proton MR microimaging and relaxation of hydrating synthetic cement pastes, in: P. Colombet, A.R. Grimmer (Eds.), Application of NMR Spectroscopy to Cement Science, Switzerland, Gordon & Breach Science Publishers, Amsterdam, 1994, pp. 353–359.

[6] A.T. Watson, C.T.P. Chang, Characterizating porous media with NMR method, Prog Nucl Magn Reson Spectrosc, 31 (1997) 343–386.

[7] H.C. Gran, E.W. Hansen, Effects of drying and freeze/thaw cycling probed by ^{1}H NMR, Cem Concr Res, 27 9 (1997) 1319–1331.

[8] F. Milia, Y. Bakopoulos, L. Milkovic, Surface induced spin-lattice relaxation of water in tricalcium silicate gels, Z Naturforsch, 46a (1991) 697–699.

[9] R. Blinc, J. Dolinsek, G. Lahajnar, A. Sepe, I. Zupanicic, S. Zumer, F. Pintar, M.M. Pintar, Spin-lattice relaxation of water in cement gels, Z Naturforsch, 43a (1988) 1026–1038.

[10] M. Bogdan, B.J. Balcom, T.W. Bremner, R.L. Armstrong, Single-point ramped imaging with T_1 enhancement (SPRITE), J Magn Reson A, 116 (1995) 266–269.

[11] S.D. Beyea, B.J. Balcom, T.W. Bremner, P.J. Prado, A.R. Cross, R.L. Grattan-Bellew, P.E. Grattan-Bellew, The influence of shrinkage–cracking on the drying behaviour of White Portland cement using Single-Point Imaging (SPI), Solid State Nucl Magn Reson, 13 1–2 (1998) 93–100.

[12] T. Nunes, E.W. Randall, A.A. Smoilenko, P. Bodart, G. Feio, The hardening of portland cement studied by ^{1}H NMR stray-field imaging, J Phys D: Appl Phys, 29 (1996) 805–808.

[13] B.J. Balcom, R.P. MacGregor, S.D. Beyea, D.P. Green, R.L. Armstrong, T.W. Bremner, Single-point ramped imaging with T_1 enhancement (SPRITE), J Magn Reson A, 123 1 (1996) 131–134.

[14] P.J. Prado, B.J. Balcom, S.D. Beyea, D.P. Green, R.L. Armstrong, T.W. Bremner, Concrete thawing studied by single-point ramped imaging, Solid State Nucl Magn Reson, 10 1–2 (1997) 1–8.

[15] P.J. Prado, B.J. Balcom, S.D. Beyea, T.W. Bremner, R.L. Armstrong, P.E. Grattan-Bellew, Concrete freeze/thaw as studied by magnetic resonance imaging, Cem Concr Res, 28 2 (1998) 261–270.

[16] W. Kurdowski, Chemia Cementu, PWN, Warszawa, 1991.

[17] P. Colombet, A.R. Grimmer, Application of NMR Spectroscopy to Cement Science, Gordon & Breach Science Publishers, Amsterdam, 1994.

[18] P. Colombet, A.R. Grimmer, H. Zanni, P. Sozanni (Eds.), Nuclear Magnetic Resonance Spectroscopy of Cement-Based Materials, Springer, Berlin, 1998.

[19] R.G. Palmer, D.L. Stein, E. Abrahams, P.W. Anderse, Models of hierarchically constrained dynamics for glassy relaxation, Phys Rev Lett, 53 (1984) 958–961.

[20] S. Gravina, D.G. Cory, Sensitivity and resolution of constant-time imaging, J Magn Reson B, 104 (1994) 53–61.